Published in final edited form as:
Aging Cell. 2013 June ; 12(3): 370–380. doi:10.1111/acel.12057.

mTOR REGULATES TAU PHOSPHORYLATION AND DEGRADATION: IMPLICATIONS FOR ALZHEIMER'S DISEASE AND OTHER TAUOPATHIES

Antonella Caccamo[1], **Andrea Magrì**[1,#], **David X. Medina**[1], **Elena V. Wisely**[1], **Manuel F. López-Aranda**[2], **Alcino J. Silva**[2], and **Salvatore Oddo**[1,*]

[1]Department of Physiology and The Barshop Institute for Longevity and Aging Studies, University of Texas Health Science Center at San Antonio. 7703 Floyd Curl Drive, San Antonio, TX 78229

[2]Departments of Neurobiology, Psychiatry and Biobehavioral Sciences, Psychology and the Brain Research Institute, University of California, Los Angeles, 695 Charles E. Young Dr South, Los Angeles, CA 90095, USA

SUMMARY

Accumulation of tau is a critical event in several neurodegenerative disorders, collectively known as tauopathies, which include Alzheimer's disease and frontotemporal dementia. Pathological tau is hyperphosphorylated and aggregates to form neurofibrillary tangles. The molecular mechanisms leading to tau accumulation remain unclear and more needs to be done to elucidate them. Age is a major risk factor for all tauopathies, suggesting that molecular changes contributing to the aging process may facilitate tau accumulation and represent common mechanisms across different tauopathies. Here, we use multiple animal models and complementary genetic and pharmacological approaches to show that the mammalian target of rapamycin (mTOR) regulates tau phosphorylation and degradation. Specifically, we show that genetically increasing mTOR activity elevates endogenous mouse tau levels and phosphorylation. Complementary to it, we further demonstrate that pharmacologically reducing mTOR signaling with rapamycin ameliorates tau pathology and the associated behavioral deficits in a mouse model overexpressing mutant human tau. Mechanistically, we provide compelling evidence that the association between mTOR and tau is linked to GSK3β and autophagy function. In summary, we show that increasing mTOR signaling facilitates tau pathology while reducing mTOR signaling ameliorates tau pathology. Given the overwhelming evidence showing that reducing mTOR signaling increases lifespan and health span, the data presented here have profound clinical implications for aging and tauopathies and provide the molecular basis for how aging may contribute to tau pathology. Additionally, these results provide pre-clinical data indicating that reducing mTOR signaling may be a valid therapeutic approach for tauopathies.

[*] *To whom correspondence should be addressed:* SALVATORE ODDO, Ph.D., Assistant Professor, Department of Physiology, University of Texas Health Science Center, San Antonio, 7703 Floyd Curl Drive, San Antonio, TX 78229-3900, Tel: 210-567-4340, Fax: 210-567-4410, oddo@uthscsa.edu.
[#]Current address: Department of Scienze Biologiche, Geologiche e Ambientali, University of Catania, viale A. Doria 6, 95125 Catania, Italy.

Author contribution

A.C. performed most of the experiments on the TSC2 mice and contributed to the manuscript preparation. A.M. performed most of the rapamycin experiments. D.X.M. measured proteasome function. E.V.W. performed some of the Western blots and edited the manuscript. M.F.A. bred and aged the TSC2 mice. A.J.S. provided intellectual contribution with the TSC2 experiments. S.O. designed the experiments, analyzed and interpreted the data and wrote the manuscript.
The authors have no conflict of interest.

Keywords

Alzheimer's disease; tauopathies; NFT; aging; rapamycin; AD; FTD; FTLD; autophagy

Introduction

Tau is a microtubule binding protein whose function is to promote microtubule assembly and stabilization. Pathological tau protein, by contrast, exhibits altered solubility properties, forms filamentous structures, and is abnormally phosphorylated at certain residues; eventually, hyperphosphorylated tau accumulates to form neurofibrillary tangles (NFTs; (Ballatore *et al.* 2007). NFTs are hallmark lesions of several neurodegenerative disorders such as Alzheimer's disease (AD), frontotemporal dementia with Parkinsonism linked to chromosome 17, Pick's disease, progressive supranuclear palsy, and corticobasal degeneration (Ballatore *et al.* 2007). Collectively, these disorders are known as tauopathies.

Overexpression of mutant human tau in rodents has been a common approach to generate animal models of tauopathies. Among these models, the P301S mice were generated by overexpressing human tau harboring the P301S mutation, which is associated with frontotemporal dementia with Parkinsonism linked to chromosome 17, under the control of the mouse prion promoter (Yoshiyama *et al.* 2007). These mice develop age-dependent accumulation of NFTs and motor dysfunction, which leads to premature death (Yoshiyama *et al.* 2007).

Despite the progress made, more needs to be done to better understand the molecular mechanisms underlying pathological tau accumulation. Age is a common event across human tauopathies; indeed, even in cases where there is a clear genetic component, tau accumulation occurs as people age (Bertram & Tanzi 2012). Similar results have been obtained in transgenic mice where usually most promoters drive expression of tau during development or shortly after birth; nevertheless, tau accumulation and the associated phenotype develops as a function of age (Bertram & Tanzi 2012). Provided this evidence, it is plausible to assume that molecular changes occurring during aging may contribute or facilitate tau accumulation. The mammalian target of rapamycin (mTOR) is a protein kinase that controls protein homeostasis by facilitating protein translation and inhibiting autophagy (Wullschleger *et al.* 2006). Overwhelming evidence has shown that reducing mTOR activity increases lifespan and health span (Harrison *et al.* 2009; Selman *et al.* 2009). It has also been reported that mTOR signaling is altered in AD brains (Chang *et al.* 2002; An *et al.* 2003; Peel & Bredesen 2003; Griffin *et al.* 2005; Pei *et al.* 2008). Specifically, the levels of mTOR and its downstream targets, including p70S6K, have been reported to be higher in human AD brains (reviewed by (Pei *et al.* 2008). We have previously shown that rapamycin, an mTOR inhibitor, ameliorates Aβ and tau pathology in the brains of 3xTg-AD mice, a widely used animal model of Alzheimer's disease (Oddo *et al.* 2003; Caccamo *et al.* 2010b; Majumder *et al.* 2011). Notably, in the 3xTg-AD mice, tau pathology is highly dependent on the accumulation of amyloid-β, another pathological hallmark of AD (Oddo *et al.* 2004; Oddo *et al.* 2006; Oddo *et al.* 2008). Thus, it remains to be established whether the rapamycin-mediated reduction of tau in these mice was due to changes in amyloid-β or to a direct interaction between mTOR and tau. Identifying whether there is a direct interaction between mTOR and tau will not only lead to a better understanding of the role of mTOR in AD, but it will also be crucial in determining the role of mTOR in other tauopathies.

Results

The tuberous sclerosis proteins (TSC) 1 and 2 are known negative regulators of mTOR (Wullschleger *et al.* 2006). Indeed, genetically reducing TSC2 causes mTOR hyperactivity in people and rodents (Onda *et al.* 1999; Prabowo *et al.* 2012). To test for a direct link between mTOR signaling and tau, we first analyzed the brains of TSC2 heterozygous mice [$TSC2^{+/-}$; (Onda *et al.* 1999)]. Specifically, we measured mTOR signaling in the hippocampi of 21-month-old $TSC2^{+/-}$ and wild type (WT) littermates (n = 6/genotype) by Western blot. mTOR activity is routinely determined by measuring the steady-state levels of p70S6K phosphorylated at Thr389 and 4E-BP1 phosphorylated at Ser65, which are two epitopes directly phosphorylated by mTOR (Guertin & Sabatini 2007; Das *et al.* 2008). Although the levels of total p70S6K were similar between $TSC2^{+/-}$ and WT mice, we found that the levels of p70S6K phosphorylated at Thr389 were significantly higher in the hippocampi of the $TSC2^{+/-}$ mice (Fig. 1A-C; $p < 0.001$ obtained by unpaired t-test analysis). Consistently, total 4E-BP1 levels were similar between the two groups, while the levels of 4E-BP1 phosphorylated at Ser65 were significantly higher in the brains of the $TSC2^{+/-}$ mice (Fig. 1A, D-E). These data are consistent with previous reports showing hyperactive mTOR signaling following reduction in TSC levels (Onda *et al.* 1999; Prabowo *et al.* 2012).

To determine the effect of genetically upregulating mTOR signaling on endogenous tau, we measured total tau levels using the mouse anti-tau antibody, Tau 5. We found that total tau levels were ~1.5 fold higher in the hippocampi of the $TSC2^{+/-}$ mice compared to age-matched WT littermates. Unpaired t-test analysis indicated that this difference was statistically significant ($p < 0.001$; Fig. 1A, F). Most notably, endogenous mouse tau was phosphorylated at Ser202/Thr205, as indicated by the AT8 antibody. Indeed, the levels of AT8-positive tau were significantly higher in the hippocampi of the $TSC2^{+/-}$ mice compared to WT littermates ($p < 0.001$; Fig. 1A, G). This is highly significant given that hyperphosphorylated tau at the AT8 sites is linked to several tauopathies (Ballatore *et al.* 2007). To begin understanding the mechanisms leading to tau phosphorylation in the $TSC2^{+/-}$ mice, we assessed whether the function of the two major tau kinases, CDK5 and GSK3β was altered. We found that the levels of CDK5 were similar between the two groups of mice (Fig. 1A, H). We then measured the steady-state levels of total and GSK3β phosphorylated at Ser9 using Western blots. GSK3β is inactive when phosphorylated at Ser9; indeed, the levels of GSK3β phosphorylated at Ser9 inversely correlate with its activity (Cohen & Goedert 2004). We found that the levels of total GSK3β were similar between $TSC2^{+/-}$ and WT mice (Fig. 1A, I). In contrast, the levels of GSK3β phosphorylated at Ser9 were significantly lower in the hippocampi of the $TSC2^{+/-}$ mice compared to WT mice ($p < 0.01$; Fig. 1A, J) strongly suggesting that GSK3β activity is upregulated in $TSC2^{+/-}$ mice. This finding is consistent with previous results that have linked mTOR and GSK3β signaling (Meske *et al.* 2008).

Overall, the data presented so far clearly show that genetic upregulation of mTOR signaling increases tau phosphorylation (via a GSK3β-mediated mechanism) and tau levels. To analyze the mechanisms underlying the increase in tau levels, we first assessed whether there is a direct transcriptional control of tau by mTOR. Toward this end, we measured tau mRNA levels using real-time PCR. We found that tau expression was similar between WT and $TSC2^{+/-}$ mice as indicated by similar threshold values (3.25 ± 0.67 and 3.48 ± 0.71 for WT and $TSC2^{+/-}$ mice, respectively). A Student's *t*-test showed that these values were not statistically significant from each other. To determine whether the increase in tau levels was due to changes in tau turnover, we focused on the two major cellular protein degradation systems, the proteasome and autophagy. First, we utilized the fluorogenic substrates Bz-VGR-AMC, Suc-LLVY-AMC and Z-LLE-AMC to measure trypsin-like, chymotrypsin-like, and PGPH activities of the proteasome in the hippocampi of $TSC2^{+/-}$ and WT mice.

We found no statistically significant changes in these activities between $TSC2^{+/-}$ and WT (Fig. 2A-C), suggesting that proteasome activity is not altered in the hippocampi of the $TSC2^{+/-}$ mice.

We next assessed whether changes in autophagy induction could account for the increase in tau levels. Toward this end, we measured the levels of the autophagy-related proteins Atg7 and the Atg5/Atg12 complex (which are necessary for autophagy induction) and LC3, which is an indicator of autophagy induction (Mizushima *et al.* 1998). Toward this end, LC3-I is post-translationally modified during autophagy induction to form LC3-II, which is incorporated into the growing autophagosome membrane (Mizushima *et al.* 1998). We found that the levels of Atg7 and the Atg5/Atg12 complex were significantly decreased in the hippocampi of $TSC2^{+/-}$ compared to WT mice ($p < 0.001$ for both; Fig. 2D-F). Furthermore, although the levels of LC3-I were similar between WT and $TSC2^{+/-}$ mice (Fig. 2D, G), the LC3-II levels were significantly lower in the hippocampi of $TSC2^{+/-}$ mice compared to WT mice ($p < 0.001$; Fig. 2D, H). Collectively, these data strongly suggest that mTOR hyperactivity leads to an increase in tau levels by reducing autophagy induction.

Further exploring the relation between mTOR and tau, we used a pharmacological approach to modulate mTOR signaling in a transgenic mouse model overexpressing human tau harboring the P301S mutation. These mice (herein referred to as P301S) develop a robust neuropathological phenotype, as described by (Yoshiyama *et al.* 2007). Specifically, these mice develop age-dependent accumulation of tau inclusions starting at 4–5 months of age. As the mice age, the tau pathology becomes more severe and is accompanied by neuronal loss around 12 months of age (Yoshiyama *et al.* 2007).

We have previously shown that rapamycin, an mTOR inhibitor, ameliorates Aβ and tau pathology in 3xTg-AD mice, a widely used animal model of Alzheimer's disease (Caccamo *et al.* 2010b; Majumder *et al.* 2011). However, it remains to be established whether the rapamycin-mediated effects on tau pathology are due to a direct link between tau and mTOR or are simply due to a decrease in Aβ levels. Toward this end, we have previously shown that decreasing Aβ levels in the 3xTg-AD mice directly affects tau pathology (Oddo *et al.* 2004; Oddo *et al.* 2006; Oddo *et al.* 2008), hence we used the P301S mice to test for a direct link between mTOR and tau. 2-month-old pre-pathological P301S mice and non-transgenic (NonTg) littermates were randomly assigned to one of the following groups (n=12 mice/group): (i) P301S mice fed rapamycin diet (P301S-Rapa); (ii) P301S fed the control diet (P301S-CTL); (iii) NonTg mice fed rapamycin diet (NonTg-Rapa); (iv) NonTg mice fed the control diet (NonTg-CTL). Mice were maintained on the appropriate diets for 6 months. The 2-month time-point was chosen because at this age the P301S mice do not show any overt pathology, which allows us to determine the effect of reducing mTOR signaling on the onset and progression of tau pathology. The rapamycin diet contained microencapsulated rapamycin at a concentration of 14.8 ng/mg. The control diet contained empty microcapsules. Importantly, these are the same formulations that have been shown to increase lifespan and ameliorate AD-like pathology in mice (Harrison *et al.* 2009; Caccamo *et al.* 2010b; Spilman *et al.* 2010; Majumder *et al.* 2011).

Mice were weighed before starting the rapamycin treatment and monthly thereafter. Notably, all four groups of mice gained weight throughout the experiments (Fig. 3A). A mixed-model, repeated-measures ANOVA indicated that there was a significant interaction between age and genotype ($p < 0.001$); however, there was no significant difference between drug treatment and genotype ($p > 0.05$). In summary, we found that the NonTg mice gained weight throughout the treatment and after 6 months of treatment, and both groups of NonTg mice weighed significantly more than the P301S mice (Fig. 3A). Notably, these changes

were linked to the genotype and were independent of rapamycin, as indicated by a post hoc test with Bonferroni correction.

At the end of the rapamycin treatment, mice were tested in a battery of cognitive and non-cognitive behavioral tasks. Mice were initially trained in the Morris water maze (MWM), a spatial learning and memory task, to find a hidden platform using extra maze cues. Escape latency data were analyzed using a mixed-model, repeated-measures ANOVA, with treatment as the categorically fixed effect, days as the numeric covariate, animals as the random effect, and escape latency as the dependent variable. We found a significant effect for days ($F = 9.585$; $p < 0.0001$), indicating that the mice significantly learned the task across sessions (Fig. 3B). However, the treatment-day interaction was not significant, indicating that all four groups of mice learned at the same pace. Taken together, we found that the P301S-CTL mice did not have any learning deficits compared to NonTg-CTL mice and that rapamycin did not enhance or diminish learning performance in P301S and NonTg mice.

The novel object recognition task was used to measure cortical and hippocampal function by observing spontaneous mouse behavior to explore a novel object (Mumby *et al.* 2002). During training mice were exposed to two objects, object A and object B, and were left free to explore for 5 minutes. As expected, mice spent the same amount of time exploring the two objects. During the probe trials, object B was replaced with a new object. We found that the NonTg-Rapa and the NonTg-CTL mice spent 71.45 ± 2.76% and 70.45 ± 3.38% of their time, respectively, exploring the new object (Fig 4C). Similarly, the P301S-Rapa and the P301S-CTL mice spent 69.03 ± 1.97 and 69.38 ± 3.34% of their time, respectively, exploring the new object (Fig. 3C). A two-way ANOVA indicated that there were no statistical differences among the groups ($p = 0.9$).

Given the motor deficits developed by the P301S mice (Yoshiyama *et al.* 2007), we next used the open-field activity test to measure general motor function. Analyses by two-way ANOVA showed a significant difference among the groups in the spontaneous activity ($p < 0.001$) and gross motor function ($p = 0.026$), as assessed by the distance covered in the activity chamber and the average speed during the test, respectively (Fig. 3D-E). We then conducted a Bonferroni's post hoc analysis to identify the group(s) responsible for the changes in spontaneous activity. We found that P301S-CTL mice performed significantly worse than the other three groups of mice ($p < 0.001$ for all comparisons). No other statistically significant differences were found indicating that the P301S-Rapa mice performed as well as the two NonTg groups (Fig. 3D). We obtained similar results when we conducted the Bonferroni's post hoc analysis on the average speed data. Specifically, we found that the P301S-CTL mice performed significantly worse than the P301S-Rapa (Fig. 3E; $p <0.05$), which performed as well as the two NonTg groups. We next assessed anxiety and stress by measuring open-field thigmotaxis and the time spent in the center of the arena. As expected, mice spent more time in the periphery compared to the center of the arena; this response was independent of the genotype or drug treatment, as no statistically significant differences were found among the different groups (Fig. 3F-G). To further evaluate motor function in the P301S mice, we tested them using the rotarod, which is widely utilized to assess motor coordination. Mice were trained for 90 seconds (6 trials/day for 3 days) on a rod at a constant speed of 15 rpm. Six 90-second probe trials were conducted on day 4 on an accelerating rod (1 rpm/sec). Analysis by two-way ANOVA showed a significant difference among the groups ($p < 0.001$; Fig. 3H). We thus conducted a Bonferroni's post hoc analysis to identify the group(s) responsible for the changes in rotarod performance. We found that the P301S-CTL mice performed significantly different compared to the other three groups ($p < 0.01$ for all comparisons; Fig. 3H). Together, these data show that the P301S mice have a

significant motor impairment, which is rescued by chronic rapamycin treatment. Indeed, the P301S-Rapa mice performed as well as the two NonTg groups.

At the end of the behavioral tests mice were 8-month-old; at this age the P301S mice show robust tau accumulation and phosphorylation. To assess the effects of rapamycin on brain tau pathology, sections from P301S-Rapa and P301S-CTL mice (n = 6/group) were immunostained with AT8, which recognizes tau phosphorylated at Ser202/Thr205. We found that the number of AT8-positive neurons was markedly reduced in the hippocampus, cortex and brain stem of P301S-Rapa mice compared to the same brain regions of P301S-CTL mice ($p < 0.01$ for all three regions; Fig. 4A-I;). To further analyze the effects of rapamycin on tau pathology, we measured the steady-state levels of soluble and insoluble tau by Western blot (n = 7/group). We found that the total levels of tau in whole brain homogenates from soluble and insoluble fractions were significantly lower in the P301S-Rapa compared to the P301S-CTL mice ($p<0.01$; Fig. 4J-K and O-P). We also found that rapamycin administration significantly reduced tau phosphorylation. Indeed, the steady-state levels of tau phosphorylated at Ser202/Thr205 (detected by the AT8-postive), Thr231/235 (detected by the AT180 antibody) and at Thr181 (detected by the AT270 antibody) were significantly lower in both soluble and insoluble fractions of rapamycin-treated transgenic mice compared to mice on the control diet ($p < 0.001$ for all comparisons except for the AT270 levels in the insoluble fraction where the p value was < 0.05; Fig. 4J, L-M and O, Q-S). We also measured tau levels in NonTg mice using the tau 5 antibody. Although we found a strong trend toward a decrease in total tau levels in the rapamycin-treated NonTg mice, the results did not reach statistical significance ($p = 0.08$; Fig. S1).

To determine whether the effects of rapamycin were mediated by mTOR, we measured mTOR signaling in the brains of P301S-Rapa and P301S-CTL mice. Although the steady-state levels of total p70S6K and 4E-BP1 were similar between treated and untreated mice, we found a significant reduction in the levels of p70S6K phosphorylated at Thr389 and 4E-BP1 phosphorylated at Ser65 in the rapamycin-treated mice compared to mice on control diet (Fig. 5A-E). Collectively, these data clearly indicate that rapamycin reaches its intended target in the brain (i.e., mTOR) and reduces its activity. Taken together, the data presented so far indicate that pharmacological reduction of mTOR signaling reduces tau pathology in the P301S transgenic mice.

To begin understanding the mechanism underlying the rapamycin-mediated reduction in tau phosphorylation, we focused on GSK3β as the data in Fig. 1 show its involvement in the mTOR tau relation. We found that while the steady-state levels of total GSK3β were similar between treated and untreated transgenic mice, the levels of GSK3β phosphorylated at Ser9 were significantly higher in the mice treated with rapamycin (Fig. 5A, F-G). Given that Ser9 is an inhibitory phospho-site, these data indicate that rapamycin decreases the activity of GSK3β.

Considering that total tau levels were also decreased by rapamycin and the involvement of protein turnover in tau pathology, we measured tau mRNA levels, we well as proteasome and autophagy function. We found that tau expression was similar between P301S-CTL and P301S-Rapa, as indicated by similar threshold values (2.08 ± 0.2 and 2.85 ± 0.2 for P301S-CTL and P301S-Rapa, respectively). A Student's *t*-test showed that these values were not statistically different from each other. Similarly, we found that overall proteasome activity was similar between P301S-CTL and P301S-Rapa mice, as indicated by the lack of statistically significant changes in the trypsin-like, chymotrypsin-like, and PGPH activities of the proteasome in the brains of these mice (Fig. 6A-C). In contrast, we found that the levels of the autophagy related proteins Atg7 and the Atg5/Atg12 complex were significantly increased in the brain of the transgenic mice receiving rapamycin (Fig. 6D-F; p

< 0.01 for both measurements). Furthermore, while the levels of LC3-I were similar between the two groups (Fig. 6D, G), the LC3-II levels were significantly increased in the brains of the P301S-Rapa mice compared to P301S-CTL mice (Fig. 6D, H; $p = 0.03$). These results are consistent with the data showing that mTOR is a negative regulator of autophagy; thus, by reducing its activity, we have observed an increase in autophagy induction.

Discussion

Tau is a microtubule-binding protein that plays a primary role in microtubule stabilization. However, growing evidence suggests that tau may have other functions in the CNS related to protein signaling and cytoskeletal organization (Morris *et al.* 2011). Tau accumulates in a group of neurodegenerative disorders known as tauopathies such as AD, frontotemporal lobar degeneration, Pick's disease, and corticobasal degeneration (Ballatore *et al.* 2007). In these disorders, tau is hyperphosphorylated and it aggregates to form insoluble inclusions that lead to the development of neurofibrillary tangles (Ballatore *et al.* 2007). Notably, recent evidence indicates that tau mediates learning and memory deficits in animal models of AD (Roberson *et al.* 2007), suggesting that reducing tau levels may represent a valid therapeutic approach.

Aging is the greatest risk factor for several neurodegenerative disorders, including tauopathies. For example, rare mutations in 3 genes have been identified as causes of AD (Bertram & Tanzi 2012). Even in these clear cut genetic cases, the penetrance of the mutations increases as a function of age. Similar observations have been reported for other tauopathies (Ballatore *et al.* 2007). However, little is known as to how aging contributes to tau accumulation. Identifying age-dependent changes in signaling pathways that could facilitate protein accumulation in the brain may offer new molecular targets for the development of new therapeutic interventions.

Overwhelming evidence from lower organisms and mammals links mTOR to aging. For example, studies from independent laboratories have shown that pharmacologically or genetically reducing mTOR signaling increases life-span and health-span in mice (Harrison *et al.* 2009; Selman *et al.* 2009). mTOR is a conserved protein kinase that plays a key role in controlling a balance between protein synthesis and degradation; indeed, mTOR dysregulation has been linked to several proteinopathies, such as Huntington's disease, AD and frontotemporal lobar degeneration (Sarkar & Rubinsztein 2008; Oddo 2012; Wang *et al.* 2012). Along these lines, we previously showed that pharmacologically reducing mTOR signaling with rapamycin ameliorates Alzheimer-like phenotype in transgenic mice and attenuates age-dependent cognitive decline in wild type mice (Caccamo *et al.* 2010b; Majumder *et al.* 2011; Majumder *et al.* 2012). Specifically, using the 3xTg-AD mice, a widely used animal model of Alzheimer's disease, we showed that reducing mTOR signaling with rapamycin was sufficient to ameliorate Aβ and tau accumulation (Griffin *et al.* 2005; Meske *et al.* 2008). However, given that the tau pathology in the 3xTg-AD mice is highly dependent on the Aβ pathology (Oddo *et al.* 2004; Oddo *et al.* 2006; Oddo *et al.* 2008), it remained to be established whether the decrease in tau in the rapamycin-treated 3xTg-AD mice was a secondary event due to a reduction of Aβ pathology or whether there was a direct link between mTOR and tau. Here we offer the first evidence in mammals of a direct link between mTOR signaling and tau accumulation. Notably, not only did we show that genetically increasing mTOR signaling increases tau levels and phosphorylation, but we also showed that reducing mTOR signaling with rapamycin ameliorates tau pathology and rescues motor deficits in a mouse model of tauopathies. Our data are consistent with in vitro data suggesting that mTOR signaling regulates tau phosphorylation (Meske *et al.* 2008) and TOR activation enhances tau-induced neurodegeneration in a *Drosophila* model of tauopathies (Khurana *et al.* 2006). Given the data presented here and the primary role of

mTOR in age-dependent proteinopathies, we propose that age-dependent accumulation of tau in proteinopathies may be linked to an increase in mTOR signaling.

mTOR dysregulation is linked to several neurogenetic disorders characterized by abnormal synaptic plasticity (Gipson & Johnston 2012). For example, mutations in the TSC1 and TSC2 genes cause mTOR hyperactivity (Prabowo *et al.* 2012) and individuals harboring those mutations develop tuberous sclerosis, an autosomal dominant disorder associated with mental retardation, autism and epilepsy (Consortium 1993); van Slegtenhorst *et al.* 1997). Most notably, tau accumulation has been reported in patients with tuberous sclerosis. Consistent with these reports, here we show that reducing TSC2 in mice leads to mTOR upregulation and tau accumulation. Together, the human data and the data presented here strongly support a role of mTOR dysregulation in tau pathology and indicate that reducing mTOR signaling may be a valid therapeutic approach for tauopathies.

Experimental procedures

Mice and rapamycin administration

The tuberous sclerosis 2 heterozygous mice and tau P301S transgenic mice used in this work were described elsewhere (Onda *et al.* 1999; Yoshiyama *et al.* 2007). P301S mice had *ad libitum* access to microencapsulated rapamycin or control diet during the treatment period.

Protein extractions

Mice were perfused with PBS, after which their brains were extracted and sagittally bisected. Half of the brain was frozen in dry ice and used for biochemical evaluation while the other half was dropped-fixed in 4% paraformaldehyde and used for histological and immunohistochemical evaluation. Where specified, the hippocampi were extracted under a dissecting scope and frozen in dry ice. Whole brain extractions were performed as previously described (Caccamo *et al.* 2010c). For hippocampal extractions, frozen hippocampi were homogenized with a dounce homogenizer in 100 μl of T-PER solution (Fisher Scientific) supplemented with protease and phosphatase inhibitors. Tissue was then centrifuged at 14,000 rpm for 49 minutes at 4 °C. The supernatant fraction was used for Western blot analyses.

Western blots, immunohistochemistry and real-time PCR

Proteins were resolved using precast SDS/PAGE gels (Invitrogen, Carlsbad, CA), as described previously (Caccamo *et al.* 2010a). Protein intensities were obtained as described in (Caccamo *et al.* 2011). For immunohistochemistry, fixed brains were sectioned using a sliding vibratome. 50 μm thick free-floating sections were stored in 0.02% sodium azide in PBS. The day of the immunostaining, sections were briefly washed with TBS (100 mM Tris pH 7.5; 150 mM NaCl) followed by a 30 minute incubation in 3% H_2O_2, to quench endogenous peroxidase activity. Next, the proper primary antibody was applied overnight at 4°C. Sections were washed 3 times in TBS and then incubated with the respective secondary antibody for 1 hour at room temperature and developed as described in (Oddo *et al.* 2007). The real-time PCR experiments were conducted as we previously described in (Caccamo *et al.* 2012).

Behavioral experiments

Mice were handled for 5 days prior the beginning of the behavioral tests. The Morris water maze was conducted in a circular plastic pool of 1.5 m in diameter. The pool was placed in a quiet room with several visual extramaze cues. Mice received 4 training trials per day for 5 consecutive days. During each training trial, mice were placed in the water until they found a platform hidden under the surface of the water, which was made opaque using non-toxic

paint. If a mouse failed to find the platform within 60 seconds, it was manually guided to the platform and allowed to remain there for 10 seconds. At the end of each trial, mice were returned to their home cages for 25 seconds. The experiments were video recorded with a camera mounted on the ceiling and scored with the EthoVision XT tracking system (Noldus biological).

The open field was performed in a clear box (40 × 40 cm) and individual mice were allowed 10 min of free exploration. The test was recorded by a camera and scored with the EthoVision XT system.

The object recognition was conducted in the same box used for the open filed task. For this paradigm, two objects were placed in the arena and mice were allowed 5 minutes of free exploration, after which they were returned to their home cage for 10 minutes. Subsequently, mice were returned to the arena; this time one of the previous objects was replaced with a new one. Data were analyzed with the EthoVision XT system.

The rotarod test was conducted as described in (Caccamo *et al.* 2012). Briefly, mice received 6 trials/day per 3 days. During this learning phase, the rod was accelerated from 0 to 15 rpm in 20 seconds and then maintained at 15 rpm for 70 seconds. Probe trials were conducted 24 hours after training and consisted of 6 sequential trials on an accelerating rod (1 rpm/sec).

Proteasomal activity

Proteasomal activity was measured as we described previously (Medina *et al.* 2011). Briefly, 10 μL of protein extracts were incubated with 75 μM proteasomal substrates Suc-LLVY-AMC, Bz-VGR-AMC and Z-LLE-AMC (Enzo Life Sciences, Plymouth Meeting, PA), which probe for chymotrypsin-like, trypsin-, and peptidylglutamyl-peptide hydrolyzing-like (PGPH) activities, respectively. Reactions were carried out in assay buffer [25 mM 4-(2-hydroxyethyl)-1-piperazineethanesulfonic acid (HEPES), pH 7.5, 0.5 mM ethylenediaminetetraacetic acid (EDTA), 0.05% NP-40] in a total of 200 mL in black 96-well plates. Kinetic readings were taken at 37°C every 1.5 minutes for 60 minutes (excitation 360 nm, emission 460 nm) using the Synergy HT microplate reader (BioTek, Winooski, VT, USA). Values were then normalized to protein concentration.

Statistical analyses

Behavioral data were analyzed by two-way ANOVA followed by a Bonferroni test to determine individual differences among groups as detailed in (Caccamo *et al.* 2010c). Student's t-test was used when suitable. Statistical evaluations were conducted with the assistance of GraphPad Prism (La Jolla, CA).

Supplementary Material

Refer to Web version on PubMed Central for supplementary material.

Acknowledgments

This work was supported by grants to S.O. from the National Institute on Aging (R01 AG037637), the Glenn Foundation and the William and Ella Owens Medical Research Foundation; and by a grant to A.J.S. from the National Institute on Mental Health (R01 MH084315). The funders had no role in study design, data collection and analysis, decision to publish, or preparation of the manuscript.

References

An WL, Cowburn RF, Li L, Braak H, Alafuzoff I, Iqbal K, Iqbal IG, Winblad B, Pei JJ. Up-regulation of phosphorylated/activated p70 S6 kinase and its relationship to neurofibrillary pathology in Alzheimer's disease. The American journal of pathology. 2003; 163:591–607. [PubMed: 12875979]

Ballatore C, Lee VM, Trojanowski JQ. Tau-mediated neurodegeneration in Alzheimer's disease and related disorders. Nature reviews. 2007; 8:663–672.

Bertram L, Tanzi RE. The genetics of Alzheimer's disease. Prog Mol Biol Transl Sci. 2012; 107:79–100. [PubMed: 22482448]

Caccamo A, Magri A, Oddo S. Age-dependent changes in TDP-43 levels in a mouse model of Alzheimer disease are linked to Abeta oligomers accumulation. Molecular neurodegeneration. 2010a; 5:51. [PubMed: 21070634]

Caccamo A, Majumder S, Oddo S. Cognitive decline typical of frontotemporal lobar degeneration in transgenic mice expressing the 25-kDa C-terminal fragment of TDP-43. The American journal of pathology. 2012; 180:293–302. [PubMed: 22067910]

Caccamo A, Majumder S, Richardson A, Strong R, Oddo S. Molecular interplay between mammalian target of rapamycin (mTOR), amyloid-beta, and Tau: effects on cognitive impairments. The Journal of biological chemistry. 2010b; 285:13107–13120. [PubMed: 20178983]

Caccamo A, Maldonado MA, Bokov AF, Majumder S, Oddo S. CBP gene transfer increases BDNF levels and ameliorates learning and memory deficits in a mouse model of Alzheimer's disease. Proceedings of the National Academy of Sciences of the United States of America. 2010c; 107:22687–22692. [PubMed: 21149712]

Caccamo A, Maldonado MA, Majumder S, Medina DX, Holbein W, Magri A, Oddo S. Naturally secreted amyloid-beta increases mammalian target of rapamycin (mTOR) activity via a PRAS40-mediated mechanism. The Journal of biological chemistry. 2011; 286:8924–8932. [PubMed: 21266573]

Chang RC, Wong AK, Ng HK, Hugon J. Phosphorylation of eukaryotic initiation factor-2alpha (eIF2alpha) is associated with neuronal degeneration in Alzheimer's disease. Neuroreport. 2002; 13:2429–2432. [PubMed: 12499843]

Cohen P, Goedert M. GSK3 inhibitors: development and therapeutic potential. Nature reviews. Drug discovery. 2004; 3:479–487.

Consortium ECTS. Identification and characterization of the tuberous sclerosis gene on chromosome 16. Cell. 1993; 75:1305–1315. [PubMed: 8269512]

Das F, Ghosh-Choudhury N, Mahimainathan L, Venkatesan B, Feliers D, Riley DJ, Kasinath BS, Choudhury GG. Raptor-rictor axis in TGFbeta-induced protein synthesis. Cellular signalling. 2008; 20:409–423. [PubMed: 18068336]

Gipson TT, Johnston MV. Plasticity and mTOR: towards restoration of impaired synaptic plasticity in mTOR-related neurogenetic disorders. Neural Plast. 2012; 2012:486402. [PubMed: 22619737]

Griffin RJ, Moloney A, Kelliher M, Johnston JA, Ravid R, Dockery P, O'Connor R, O'Neill C. Activation of Akt/PKB, increased phosphorylation of Akt substrates and loss and altered distribution of Akt and PTEN are features of Alzheimer's disease pathology. Journal of neurochemistry. 2005; 93:105–117. [PubMed: 15773910]

Guertin DA, Sabatini DM. Defining the role of mTOR in cancer. Cancer cell. 2007; 12:9–22. [PubMed: 17613433]

Harrison DE, Strong R, Sharp ZD, Nelson JF, Astle CM, Flurkey K, Nadon NL, Wilkinson JE, Frenkel K, Carter CS, Pahor M, Javors MA, Fernandez E, Miller RA. Rapamycin fed late in life extends lifespan in genetically heterogeneous mice. Nature. 2009; 460:392–395. [PubMed: 19587680]

Khurana V, Lu Y, Steinhilb ML, Oldham S, Shulman JM, Feany MB. TOR-mediated cell-cycle activation causes neurodegeneration in a Drosophila tauopathy model. Curr Biol. 2006; 16:230–241. [PubMed: 16461276]

Majumder S, Caccamo A, Medina DX, Benavides AD, Javors MA, Kraig E, Strong R, Richardson A, Oddo S. Lifelong rapamycin administration ameliorates age-dependent cognitive deficits by reducing IL-1beta and enhancing NMDA signaling. Aging Cell. 2012; 11:326–335. [PubMed: 22212527]

Majumder S, Richardson A, Strong R, Oddo S. Inducing autophagy by rapamycin before, but not after, the formation of plaques and tangles ameliorates cognitive deficits. PloS one. 2011; 6:e25416. [PubMed: 21980451]

Medina DX, Caccamo A, Oddo S. Methylene blue reduces abeta levels and rescues early cognitive deficit by increasing proteasome activity. Brain pathology. 2011; 21:140–149. [PubMed: 20731659]

Meske V, Albert F, Ohm TG. Coupling of mammalian target of rapamycin with phosphoinositide 3-kinase signaling pathway regulates protein phosphatase 2A- and glycogen synthase kinase-3-dependent phosphorylation of Tau. The Journal of biological chemistry. 2008; 283:100–109. [PubMed: 17971449]

Mizushima N, Noda T, Yoshimori T, Tanaka Y, Ishii T, George MD, Klionsky DJ, Ohsumi M, Ohsumi Y. A protein conjugation system essential for autophagy. Nature. 1998; 395:395–398. [PubMed: 9759731]

Morris M, Maeda S, Vossel K, Mucke L. The many faces of tau. Neuron. 2011; 70:410–426. [PubMed: 21555069]

Mumby DG, Gaskin S, Glenn MJ, Schramek TE, Lehmann H. Hippocampal damage and exploratory preferences in rats: memory for objects, places, and contexts. Learn Mem. 2002; 9:49–57. [PubMed: 11992015]

Oddo S. The role of mTOR signaling in Alzheimer disease. Front Biosci (Schol Ed). 2012; 4:941–952. [PubMed: 22202101]

Oddo S, Billings L, Kesslak JP, Cribbs DH, LaFerla FM. Abeta immunotherapy leads to clearance of early, but not late, hyperphosphorylated tau aggregates via the proteasome. Neuron. 2004; 43:321–332. [PubMed: 15294141]

Oddo S, Caccamo A, Cheng D, Jouleh B, Torp R, LaFerla FM. Genetically augmenting tau levels does not modulate the onset or progression of Abeta pathology in transgenic mice. Journal of neurochemistry. 2007; 102:1053–1063. [PubMed: 17472708]

Oddo S, Caccamo A, Shepherd JD, Murphy MP, Golde TE, Kayed R, Metherate R, Mattson MP, Akbari Y, LaFerla FM. Triple-transgenic model of Alzheimer's disease with plaques and tangles: intracellular Abeta and synaptic dysfunction. Neuron. 2003; 39:409–421. [PubMed: 12895417]

Oddo S, Caccamo A, Tseng B, Cheng D, Vasilevko V, Cribbs DH, LaFerla FM. Blocking Abeta42 accumulation delays the onset and progression of tau pathology via the C terminus of heat shock protein70-interacting protein: a mechanistic link between Abeta and tau pathology. J Neurosci. 2008; 28:12163–12175. [PubMed: 19020010]

Oddo S, Vasilevko V, Caccamo A, Kitazawa M, Cribbs DH, LaFerla FM. Reduction of soluble Abeta and tau, but not soluble Abeta alone, ameliorates cognitive decline in transgenic mice with plaques and tangles. The Journal of biological chemistry. 2006; 281:39413–39423. [PubMed: 17056594]

Onda H, Lueck A, Marks PW, Warren HB, Kwiatkowski DJ. Tsc2(+/−) mice develop tumors in multiple sites that express gelsolin and are influenced by genetic background. The Journal of clinical investigation. 1999; 104:687–695. [PubMed: 10491404]

Peel AL, Bredesen DE. Activation of the cell stress kinase PKR in Alzheimer's disease and human amyloid precursor protein transgenic mice. Neurobiology of disease. 2003; 14:52–62. [PubMed: 13678666]

Pei JJ, Bjorkdahl C, Zhang H, Zhou X, Winblad B. p70 S6 kinase and tau in Alzheimer's disease. J Alzheimers Dis. 2008; 14:385–392. [PubMed: 18688088]

Prabowo AS, Anink JJ, Lammens M, Nellist M, van den Ouweland AM, Adle-Biassette H, Sarnat HB, Flores-Sarnat L, Crino PB, Aronica E. Fetal Brain Lesions in Tuberous Sclerosis Complex: TORC1 Activation and Inflammation. Brain pathology. 2012

Roberson ED, Scearce-Levie K, Palop JJ, Yan F, Cheng IH, Wu T, Gerstein H, Yu GQ, Mucke L. Reducing endogenous tau ameliorates amyloid beta-induced deficits in an Alzheimer's disease mouse model. Science (New York, N.Y. 2007; 316:750–754.

Sarkar S, Rubinsztein DC. Huntington's disease: degradation of mutant huntingtin by autophagy. Febs J. 2008; 275:4263–4270. [PubMed: 18637946]

Selman C, Tullet JM, Wieser D, Irvine E, Lingard SJ, Choudhury AI, Claret M, Al-Qassab H, Carmignac D, Ramadani F, Woods A, Robinson IC, Schuster E, Batterham RL, Kozma SC,

Thomas G, Carling D, Okkenhaug K, Thornton JM, Partridge L, Gems D, Withers DJ. Ribosomal protein S6 kinase 1 signaling regulates mammalian life span. Science (New York, N.Y. 2009; 326:140–144.

Spilman P, Podlutskaya N, Hart MJ, Debnath J, Gorostiza O, Bredesen D, Richardson A, Strong R, Galvan V. Inhibition of mTOR by rapamycin abolishes cognitive deficits and reduces amyloid-beta levels in a mouse model of Alzheimer's disease. PloS one. 2010; 5:e9979. [PubMed: 20376313]

van Slegtenhorst M, de Hoogt R, Hermans C, Nellist M, Janssen B, Verhoef S, Lindhout D, van den Ouweland A, Halley D, Young J, Burley M, Jeremiah S, Woodward K, Nahmias J, Fox M, Ekong R, Osborne J, Wolfe J, Povey S, Snell RG, Cheadle JP, Jones AC, Tachataki M, Ravine D, Sampson JR, Reeve MP, Richardson P, Wilmer F, Munro C, Hawkins TL, Sepp T, Ali JB, Ward S, Green AJ, Yates JR, Kwiatkowska J, Henske EP, Short MP, Haines JH, Jozwiak S, Kwiatkowski DJ. Identification of the tuberous sclerosis gene TSC1 on chromosome 9q34. Science (New York, N.Y. 1997; 277:805–808.

Wang IF, Guo BS, Liu YC, Wu CC, Yang CH, Tsai KJ, Shen CK. Autophagy activators rescue and alleviate pathogenesis of a mouse model with proteinopathies of the TAR DNA-binding protein 43. Proceedings of the National Academy of Sciences of the United States of America. 2012; 109:15024–15029. [PubMed: 22932872]

Wullschleger S, Loewith R, Hall MN. TOR signaling in growth and metabolism. Cell. 2006; 124:471–484. [PubMed: 16469695]

Yoshiyama Y, Higuchi M, Zhang B, Huang SM, Iwata N, Saido TC, Maeda J, Suhara T, Trojanowski JQ, Lee VM. Synapse loss and microglial activation precede tangles in a P301S tauopathy mouse model. Neuron. 2007; 53:337–351. [PubMed: 17270732]

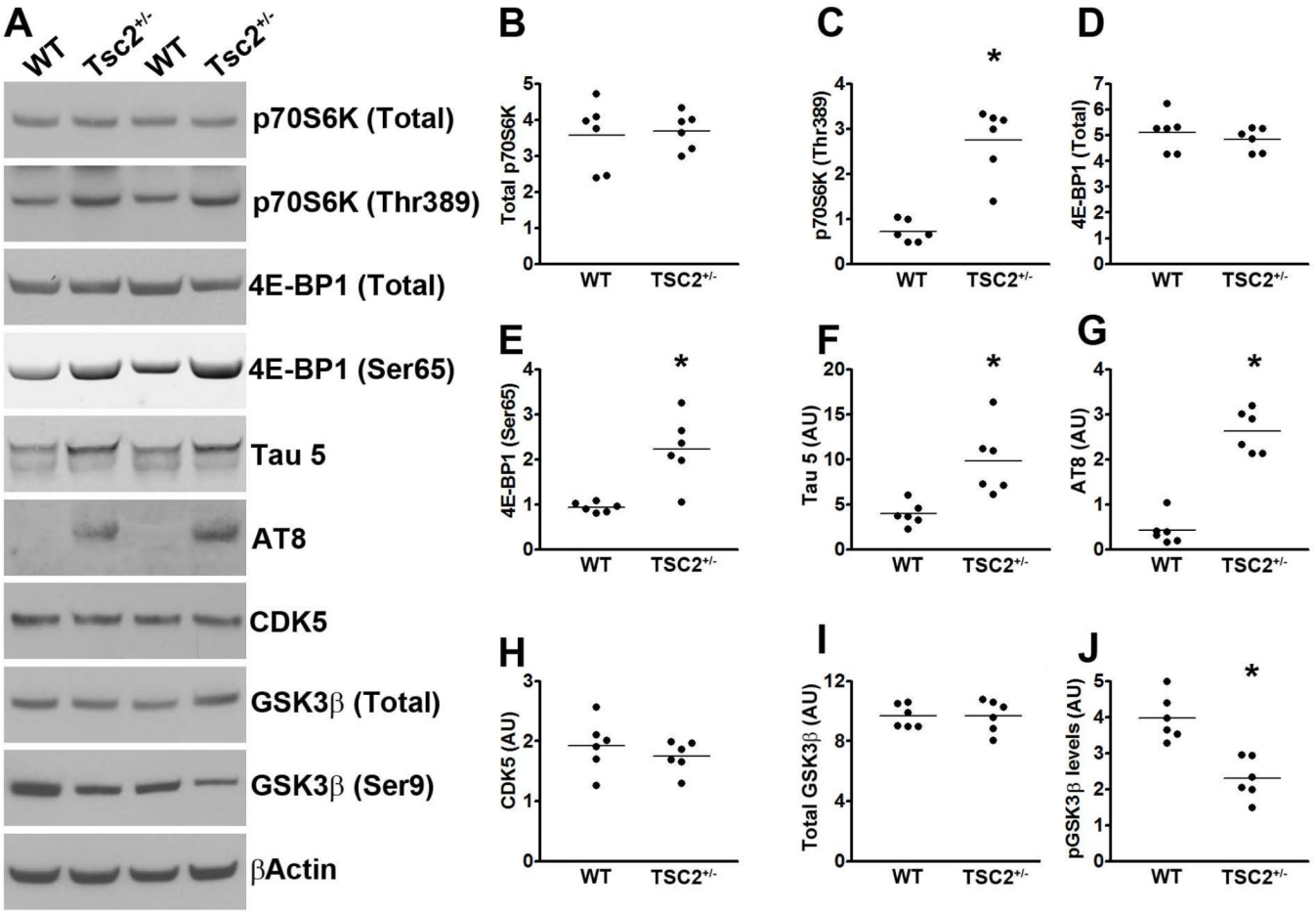

Figure 1. mTOR signaling inversely correlates with Tau levels and phosphorylation in TSC2$^{+/-}$ mice

(A) Western blots of proteins extracted from the hippocampi of TSC2$^{+/-}$ mice and WT littermates, and probed with the indicated antibodies. **(B-C)** Quantitative analyses of total and phosphorylated p70S6K, respectively. Statistical analyses show that the levels of p70S6K phosphorylated at Thr389 were significantly higher in the hippocampi of the TSC2$^{+/-}$ mice compared to WT littermates. **(D-E)** Quantitative analyses of total and phosphorylated 4E-BP1, respectively, showed that the levels of 4E-BP1 phosphorylated at Ser65 were significantly higher in the hippocampi of the TSC2$^{+/-}$ mice compared to WT littermates. **(F-G)** Quantitative analyses of total (detected by the tau 5 antibody) and phosphorylated (detected by the AT8 antibody) tau showed that endogenous mouse levels were significantly higher in the hippocampi of the TSC2$^{+/-}$ mice compared to WT littermates. **(H)** Quantitative analyses of the CDK5 band showed no differences between the two groups of mice. **(I-J)** Quantitative analyses of the total and phospho-GSK3β bands, respectively. Statistical analyses indicated no changes in total GSK3β levels between the two groups. In contrast, the levels of GSK3β phosphorylated at Ser9 were significantly lower in the hippocampi of the TSC2$^{+/-}$ mice. Quantifications of the Western blots were done by normalizing the protein of interest to β-actin, which was used as a loading control. Data are presented as means ± SEM and analyzed by student's t-test.

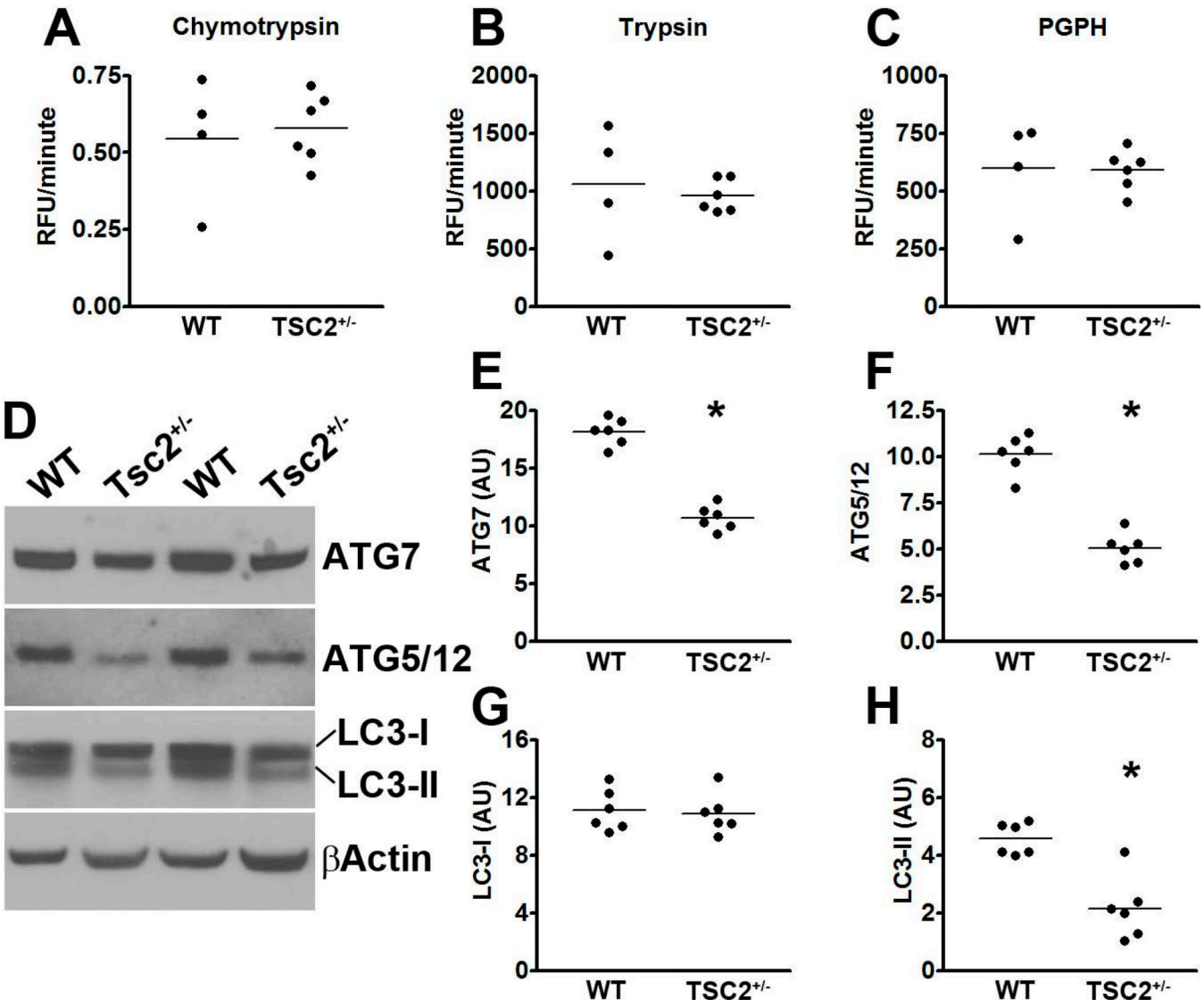

Figure 2. Autophagy induction is decreased in the brains of TSC2$^{+/-}$ mice

(A-C) Hippocampi homogenates from TSC2$^{+/-}$ and WT littermates were analyzed for proteasome activity. The data show that removing one TSC2 allele did not alter the chymotrypsin- and trypsin- like activities, nor did it change the peptidylglutamyl-peptide hydrolyzing (PDPH) activity. **(D)** Western blots of proteins extracted from the hippocampi of TSC2$^{+/-}$ mice and WT littermates. **(E-H)** Quantitative analyses of the blots show that the levels of the autophagy related proteins Atg7 (E) and Atg5/12 (F) were significantly decreased in TSC2$^{+/-}$ mice. Further, while quantitative analyses of the LC3-I levels showed no differences between the two groups of mice (G), LC3-II levels were significantly lower in the hippocampi of TSC2$^{+/-}$ mice compared to WT littermates (H). Quantifications of the Western blots were done by normalizing the protein of interest to β-actin, which was used as a loading control. Data are presented as means ± SEM and analyzed by student's t-test.

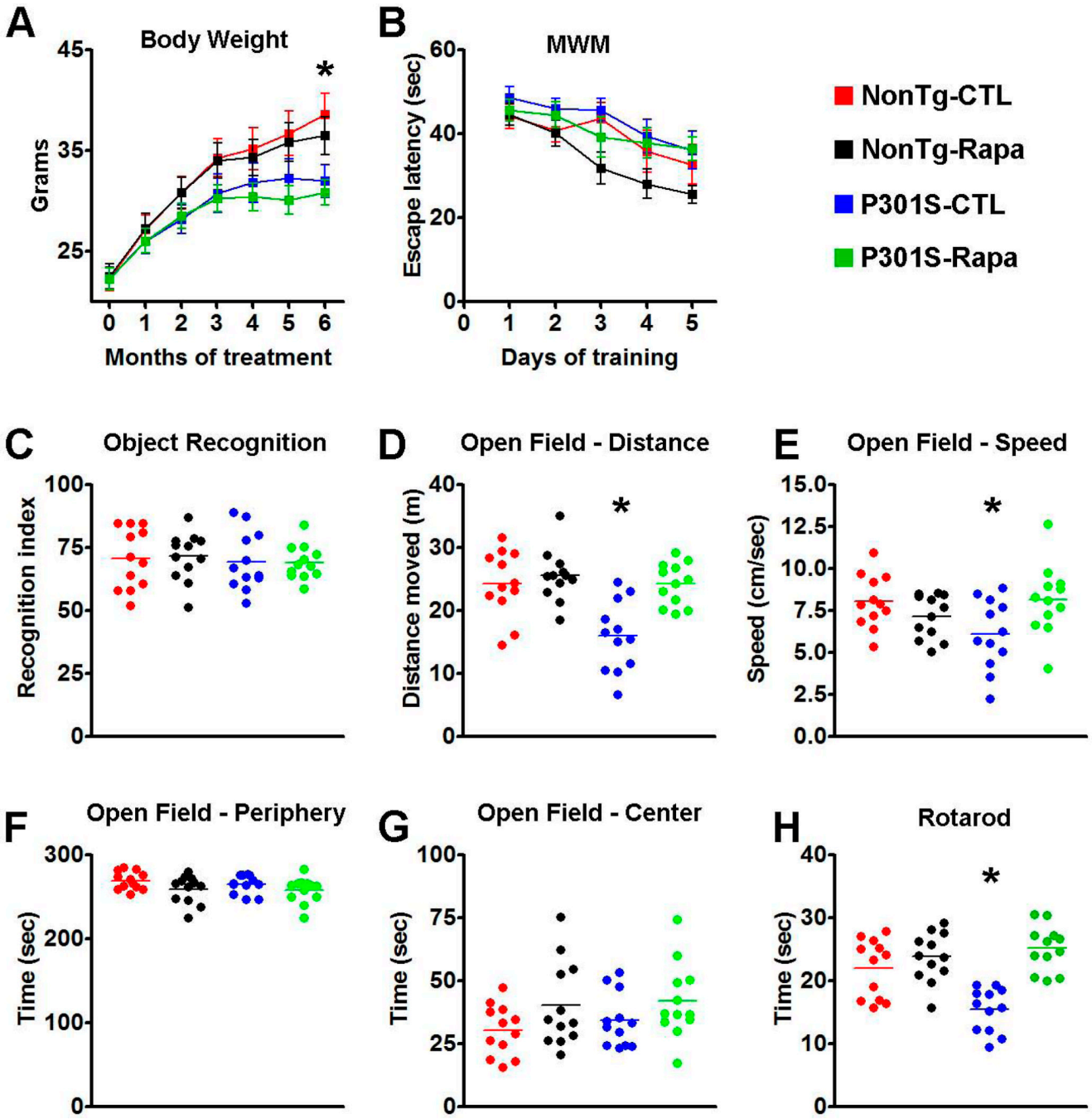

Figure 3. Rapamycin improves motor deficits in P301S mice

(A) Transgenic P301S and NonTg mice were treated with rapamycin for 6 months. The graph shows the average body weight for each group of mice, measured monthly. Notably, the body weight of the P301S mice starts to plateau after 4 months of treatment while the WT mice gain weight throughout the treatment period. Statistical analyses indicated that this difference was linked to the genotype and was independent of rapamycin administration. **(B)** Learning curve depicting mice performance in the Morris water maze. All mice significantly learned the task over the 5 days of training, as indicated by a reduced time to find the escape platform; however, no statistically significant changes were detected among the groups. **(C)**

Novel object recognition tests, a behavioral task highly dependent on the cortex, shows no differences among the 4 groups of mice. The graph depicts the recognition index, i.e., the percentage of exploration time that mice spend exploring the new object. **(D-G)** Open field activity measures spontaneous activity and anxiety. The data show that during the test, the P301S mice moved less (D) and at a slower speed (E) compared to the other three groups of mice. These changes were statistically significant. In contrast, no differences among the groups were found when measuring the time spent in the periphery and center of the arena (F and G, respectively), indicating that the P301S mice had no detectable anxiety defects and that rapamycin did not alter this normal condition. **(H)** The graph shows data obtained with the accelerating rotarod. Statistical evaluation indicated that the P301S-CTL mice were significantly impaired in this task and that rapamycin administration rescued this motor deficit. Indeed, the P301S-Rapa mice performed as well as the two NonTg groups. Data are presented as means ± SEM and were analyzed by two-way ANOVA followed by a Bonferroni test to determine individual differences among groups.

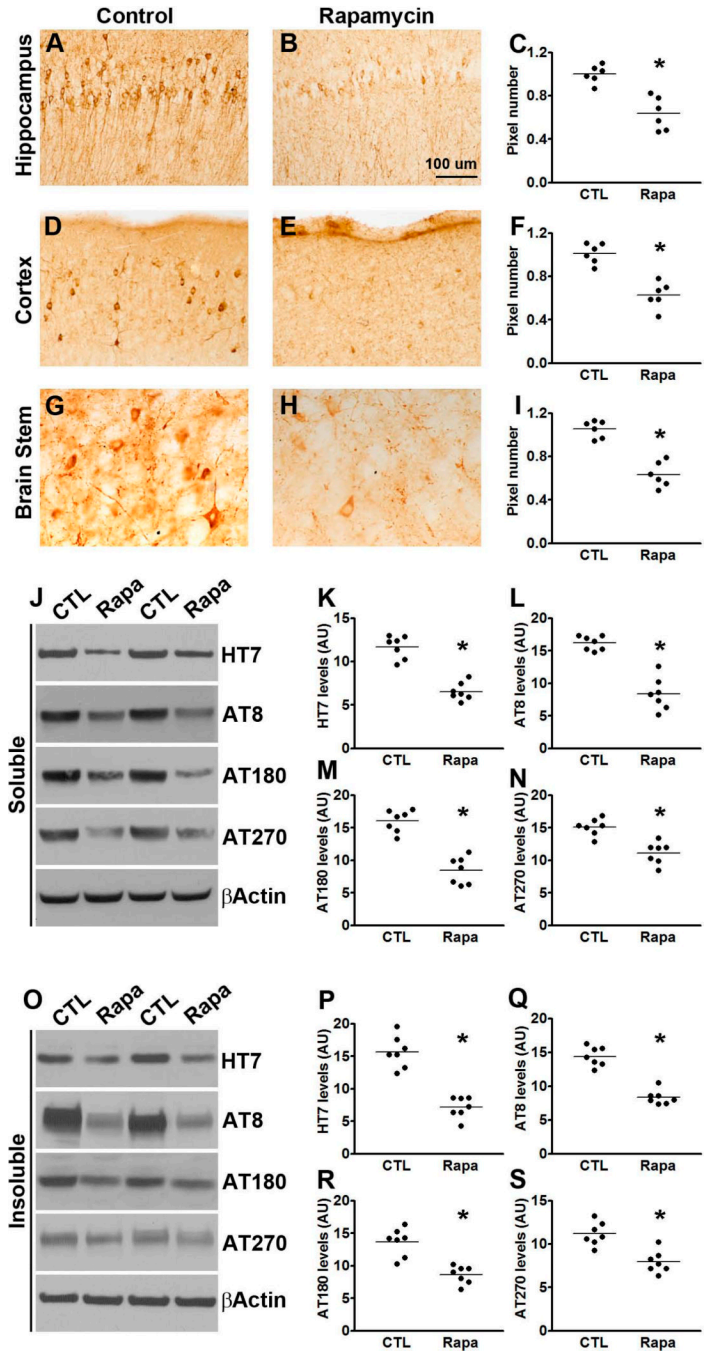

Figure 4. Rapamycin decreases tau pathology in P301S mice

(A-I) Microphotographs and quantitative analyses of P301S mice treated with rapamycin or control diet and stained with the AT8 antibody. **(J)** Western blots of soluble tau extracted from the brains of P301S mice treated with rapamycin or control diet and probed with the indicated antibodies. **(F-H)** Quantitative analyses of the blots show that rapamycin treatment significantly decreased the levels of tau phosphorylated at the AT8, AT180 and AT270 epitopes. **(O)** Western blots of insoluble tau extracted from the brains of P301S mice treated with rapamycin or control diet and probed with the indicated antibodies. **(P-S)** Quantitative analyses of the blots show that rapamycin significantly decreased the levels of tau

phosphorylated at the AT8, AT180 and AT270 epitopes. Quantifications of the Western blots were done by normalizing the protein of interest to β-actin, which was used as a loading control. Data are presented as means ± SEM and analyzed by student's t-test.

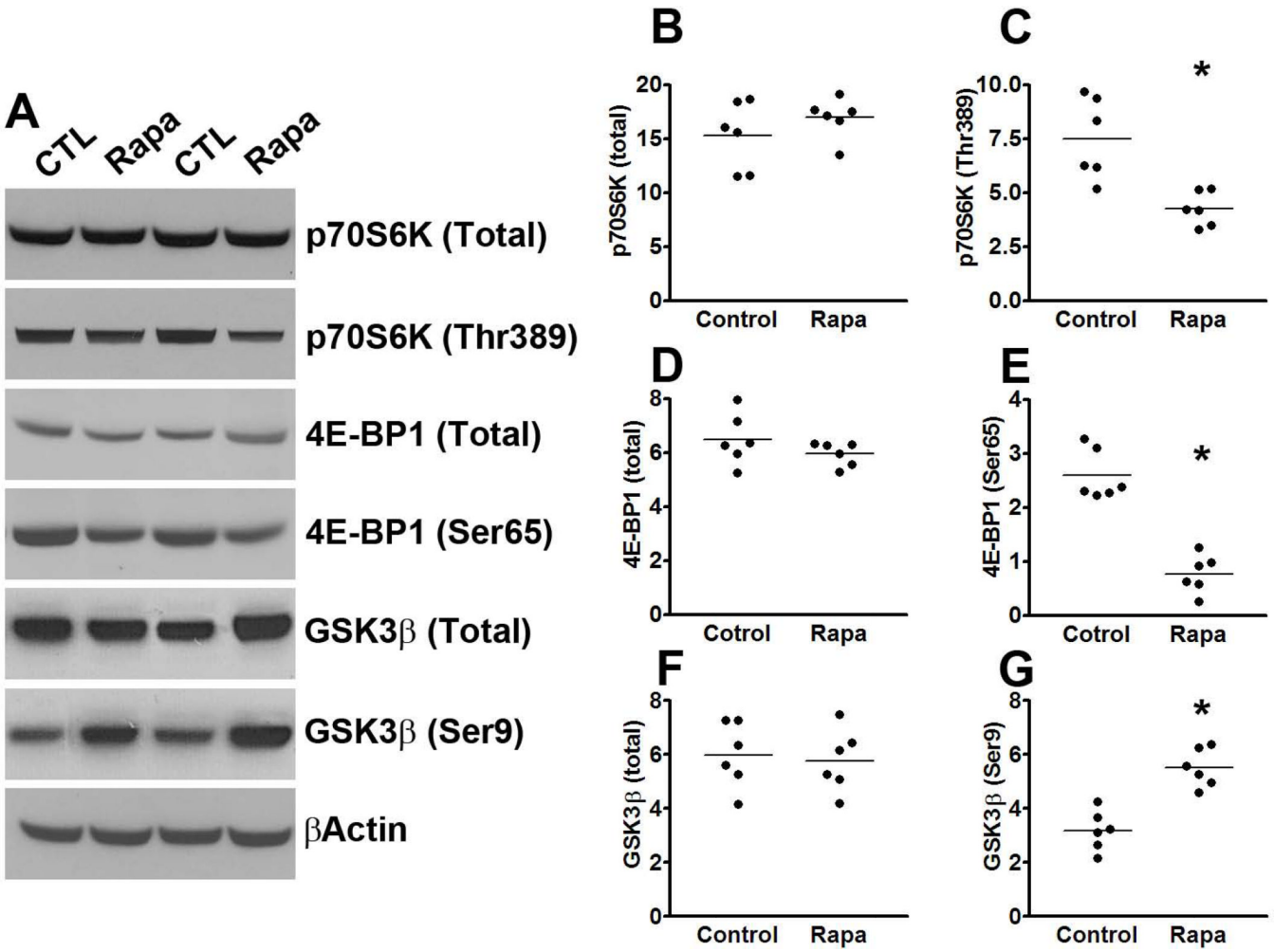

Figure 5. mTOR signaling is decreased in P301S mice treated with rapamycin

(A) Western blots of proteins extracted from the brains of P301S mice treated with rapamycin or control diet and probed with the indicated antibodies. **(B-E)** Quantitative analyses of the blots show that the levels of p70S6K phosphorylated at Thr389 and 4E-BP1 phosphorylated at Ser65 were significantly lower in the rapamycin treated mice compared to the mice on control diet. **(F-G)** Quantitative analyses of the blots show that the levels of GSK3β were significantly lower in the rapamycin treated mice compared to the mice on control diet, while no difference was detected for total GSK3β levels. Quantifications of the Western blots were done by normalizing the protein of interest to β-actin, which was used as a loading control. Data are presented as means ± SEM and analyzed by student's t-test.

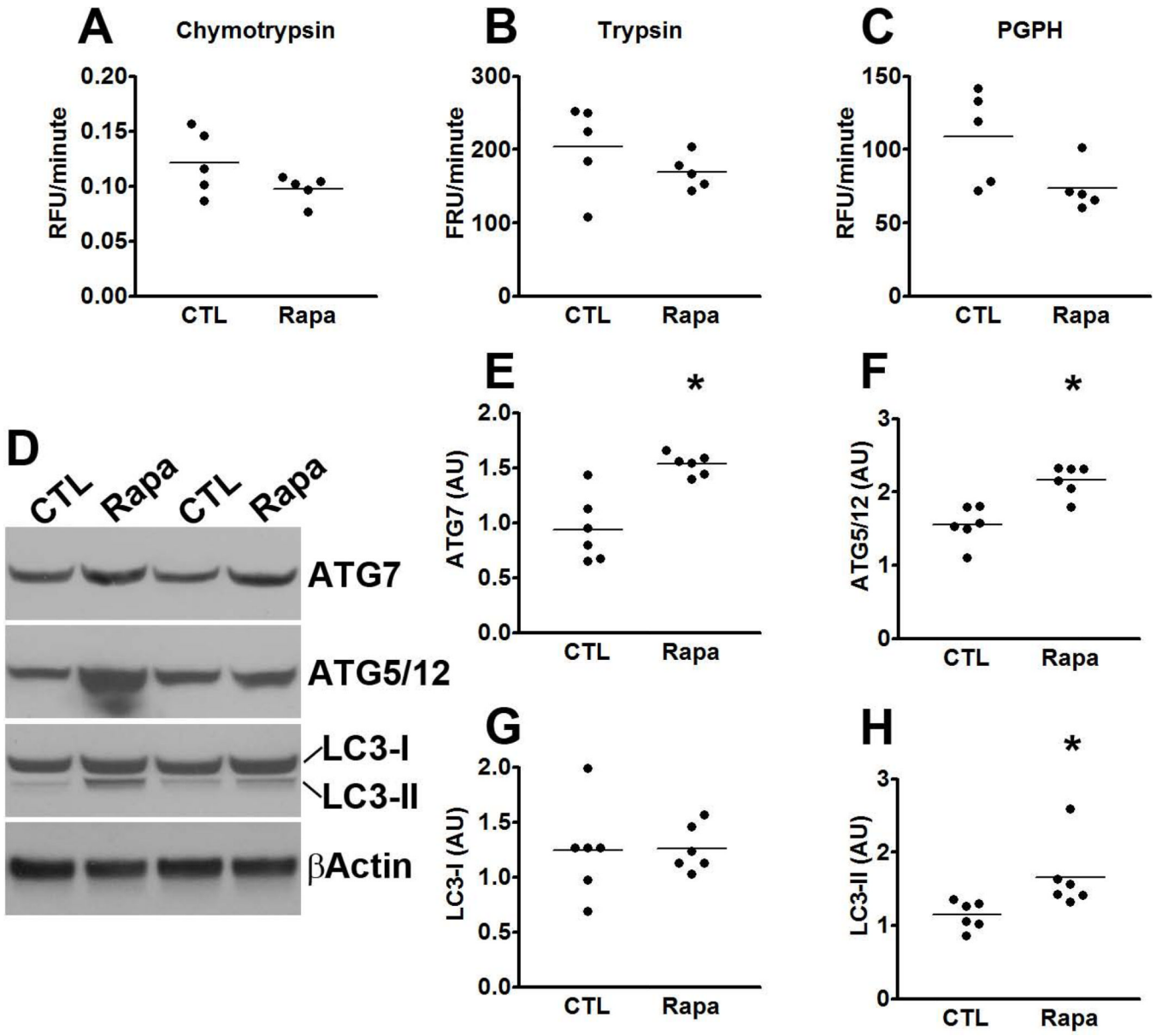

Figure 6. Autophagy induction is increased in the brains of rapamycin-treated P301S mice

(A-C) Brain homogenates from rapamycin- and control-treated P301S mice were analyzed for proteasome activity. The data show that rapamycin did not alter the chymotrypsin- and trypsin- like activities, nor did it change the peptidylglutamyl-peptide hydrolyzing (PDPH) activity. **(D)** Representative Western blots of proteins extracted from the brains of P301S mice treated with rapamycin or control diet. **(E-H)** Quantitative analyses of the blots show that the levels of the autophagy related proteins Atg7 (E) and Atg5/12 (F) were significantly increased in the P301S mice treated with rapamycin. While quantitative analyses of the LC3-I levels showed no differences between the two groups of mice (G), LC3-II levels were significantly higher in the rapamycin-treated P301S mice (H). Quantifications of the Western blots were done by normalizing the protein of interest to β-actin, which was used as a loading control. Data are presented as means ± SEM and analyzed by student's t-test.